Video Article

A Fabrication and Measurement Method for a Flexible Ferroelectric Element Based on Van Der Waals Heteroepitaxy

Jie Jiang*[1], Yugandhar Bitla*[2], Qiang-xiang Peng[1], Yi-Chun Zhou[1], Ying-Hao Chu[3]

[1]Key Laboratory of Low Dimensional Materials and Application Technology of Ministry of Education, Xiangtan University

[2]Department of Physics, Indian Institute of Science

[3]Department of Materials Science and Engineering, National Chiao Tung University

*These authors contributed equally

Correspondence to: Yi-Chun Zhou at zhouyc@xtu.edu.cn, Ying-Hao Chu at yhc@nctu.edu.tw

URL: https://www.jove.com/video/57221
DOI: doi:10.3791/57221

Keywords: Engineering, Issue 134, Flexible electronics, flexible nonvolatile memory, muscovite mica, van der Waals epitaxy

Date Published: 4/8/2018

Citation: Jiang, J., Bitla, Y., Peng, Q.x., Zhou, Y.C., Chu, Y.H. A Fabrication and Measurement Method for a Flexible Ferroelectric Element Based on Van Der Waals Heteroepitaxy. *J. Vis. Exp.* (134), e57221, doi:10.3791/57221 (2018).

Abstract

Flexible non-volatile memories have received much attention as they are applicable for portable smart electronic device in the future, relying on high-density data storage and low-power consumption capabilities. However, the high-quality oxide based nonvolatile memory on flexible substrates is often constrained by the material characteristics and the inevitable high-temperature fabrication process. In this paper, a protocol is proposed to directly grow an epitaxial yet flexible lead zirconium titanate memory element on muscovite mica. The versatile deposition technique and measurement method enable the fabrication of flexible yet single-crystalline non-volatile memory elements necessary for the next generation of smart devices.

Video Link

The video component of this article can be found at https://www.jove.com/video/57221/

Introduction

The successful fabrication of flexible nonvolatile memory elements (NVME) plays a key role in exploiting the full potential of flexible electronics. NVME shall feature light weight, low cost, low-power consumption, fast speed and high storage density capabilities besides data storage, information processing and communication. Perovskite Pb $(Zr,Ti)O_3$ (PZT) acts as a popular system for such applications considering its large polarization, fast polarization switching, high Curie temperature, low coercive field and high piezoelectric coefficient. In ferroelectric nonvolatile memories, an external voltage pulse can switch the two remnant polarizations between two stable directions, represented by '0' and '1'. It is non-volatile, and the write/read process can be completed within nanoseconds. NVME based on organic[1,2,3,4,5,6] and inorganic[7,8,9,10,11,12,13,14,15] ferroelectric materials have been attempted on flexible substrates. However, such integration is limited by not only the substrates' inability of high-temperature growth but also the degraded device performance, current leakage and electrical shorting due to their rougher surfaces. Despite promising results, alternate strategies like the thinning of substrate[8] and the epitaxial layer transfer on a flexible substrate[15] suffer restricted viability in view of the sophisticated multistep process, the unpredictability of transfer, and the limited applicability.

For the aforementioned reasons, it is critical to explore an appropriate substrate that is able to overcome limited thermal and operational stabilities of soft substrates to further advance flexible electronics. A natural muscovite mica $(KAl_2(AlSi_3O_{10})(OH)_2)$ substrate with unique features like atomically smooth surfaces, high thermal stability, chemical inertness, high transparency, mechanical flexibility, and compatibility with current fabrication methods can be used to effectively deal with these issues. More so, the two-dimensional layered structure of monoclinic mica supports van der Waals epitaxy, which mitigates lattice and thermal matching conditions, thereby significantly suppressing the substrate clamping effect. These advantages have been exploited in the direct growth of functional oxides[16,17,18,19,20,21,22,23] on muscovite recently, in view of flexible device applications.

Herein, we describe a protocol to directly grow epitaxial yet flexible lead zirconium titanate (PZT) thin films on muscovite mica. This is achieved through a pulsed laser deposition process relying on the versatile properties of mica, resulting in van der Waals heteroepitaxy. Such fabricated structures retain all the superior properties of epitaxial PZT on rigid single crystalline substrates and exhibits excellent thermal and mechanical stabilities. This simple and reliable approach provides a technological advantage over multistep-transfer and substrate thinning strategies and facilitates the development of much-awaited flexible yet single-crystalline non-volatile memory elements prerequisite for next-generation smart devices with high performance.

Protocol

1. Fabricating Flexible PZT Thin Films

1. Cut a 1 cm x 1 cm mica substrate from a mica sheet with scissors.
2. Fix this 1 cm x 1 cm mica substrate on a desk using double-sided tape.
3. Use tweezers to peel-off the mica layer-by-layer until the desired thickness (50 µm), measured with a micrometer.
4. Paste this freshly cleaved mica substrate on a 5" substrate holder using a thin layer of silver paint and cure it at 120 °C on a hot plate for 10 minutes to affix mica on substrate firmly.
5. Put the PLD (Pulsed Laser Deposition) substrate holder into the PLD chamber.
6. Select the repetition rate (*e.g.*, 10 Hz) and laser energy (*e.g.*, 300 mJ).
7. Move the focusing lens to the set position.
8. Open the shutter and deposit a 5 nm $CoFe_2O_4$ (CFO) [Laser energy: 300 mJ, Oxygen pressure: 50 mTorr, Sample temperature: 590 °C, Deposition time: 5 min] thin film as a buffer layer by triggering the laser (**Figure 1**).
9. Deposit a 20-80 nm $SrRuO_3$ (SRO) [Laser energy: 300 mJ, Oxygen pressure: 100 mTorr, Sample temperature: 680 °C, Deposition time: 10-30 min] on the CFO buffer layer as the bottom electrode for subsequent electrical performance tests by triggering the laser (**Figure 1**).
10. Deposit a 150 nm PZT [Laser energy: 300 mJ, Oxygen pressure: 100 mTorr, Sample temperature: 650 °C, Deposition time: 60 min] thin film on the top of SRO bottom electrode by triggering the laser (**Figure 1**).
11. Vent the chamber using N_2 and remove the PZT/mica sample (**Figure 2**) when the temperature reaches room temperature.
12. Put the sample on a piece of glass.
13. Put a predesigned mesh with 200 µm diameter on top of the sample. Fix the mesh well and put mesh-sample into the sputtering chamber.
14. Use DC sputtering (10 mA, 8 mbar, 6 min) to deposit Pt top electrodes on the film. Remove the sample after the sputtering.
15. Use a knife or 20% HF acid to remove a 1 mm x 1 mm PZT section. This is to uncover the bottom SRO electrode and form many small flexible ferroelectric capacitors.
    NOTE: Grow SRO as the bottom electrode, and then deposit Pt on top of the electrodes on the films by DC sputtering to form many small capacitors to measure the electronic properties of the PZT thin film, which is shown in **Figure 3**.
16. Paint a coat of conductive silver on the exposed SRO to increase the electrical conductivity of the bottom SRO electrode. Ensure that the conductive silver can contact the exposed SRO.

2. Ferroelectric Characterization

1. Bending Test
    1. On the backside of the flexible sample, glue a piece of paper with the same size as the sample for easy transfer of the sample from one stage to another.
    2. Place the PZT/mica on the test board of the ferroelectric test system and semiconductor device analyzer.
    3. Put one measurement probe of the ferroelectric test system and semiconductor device analyzer on the Pt top electrode and put the other measurement probe on the silver-SRO layer to get the polarization-electric field (P-E) hysteresis loops and capacitance-electric field (C-E) curves while the sample is unbent.
        1. Measure the P-E hysteresis loops with the two probes at a 2 kHz frequency and at 4 V. Measure the C-E curves with the two probes at a 1 MHz frequency and at 4 V. Remove the unbent sample.
    4. Secure the flexible PZT/mica thin film on the desired mold using double-sided tape. Take care to avoid the slipping/gliding of mica during the measurement.
    5. Mount it on the test board of the ferroelectric test system and semiconductor device analyzer.
    6. Put one probe on the Pt top electrode while the other probe touches the bottom SRO electrode through the silver coating similar to the configuration used earlier (step 2.1.3).
    7. Measure the P-E hysteresis loops and C-E curves under various tensile and compressive bending radii (**Figure 4**).
        1. Measure the P-E hysteresis loops with the two probes at a 2 kHz frequency and at 4 V. Measure the C-E curves with the two probes at a 1 MHz frequency and at 4 V.
    8. Remove the flexible PZT sample when the P-E and C-E measurements are completed.
2. Thermal Stability
    1. Put the PZT/mica on the test board of the ferroelectric test system and semiconductor device analyzer.
    2. Put one measurement probe on the Pt top electrode and put the other measurement probe on the silver-SRO layer.
    3. Open the temperature control system to heat the sample.
    4. Conduct the P-E and C-E measurements at different temperatures (25 °C, 50 °C, 75 °C, 100 °C, 125 °C, 150 °C, 175 °C).
    5. Turn off the heater assembly after the measurements are done.
3. Bending cyclability tests
    1. Mount the flexible PZT/mica into the two grooves of this setup.
    2. Fix one end of the sample while it is bent from the other end with the aid of a motor.
    3. Use a ruler to measure the PZT/mica length along with the movement (bending) direction of the motor prior to the 8 mm bending process (**Figure 5**).
    4. Calculate the movement length C to bend the sample 5 mm according to the formula: C=L-2Rsin(L/2R), where L is the length of PZT/mica in unbent state, R is the bending radii, and C is the movement length of the motor.
    5. Set number of bending cycles (1000) in the computer (**Figure 6**).

6. Click the Start button (**Figure 6**) to initiate the back and forth motor motion.
7. Remove the sample and measure the P-E to check whether the ferroelectric properties are retained.

Representative Results

The epitaxial PZT/SRO/CFO/mica thin films were deposited with the pulsed laser deposition technique as outlined in Step 1. **Figure 1** shows the growth scheme and **Figure 2** shows an actual flexible NVM element based on the PZT.

Mechanical stability is a crucial aspect of flexible device application. The macroscopic ferroelectric performance of the heterostructure against mechanical flexing was evaluated under both tensile and compressive bending. **Figure 7a and 7b** show the P-E and C-E hysteresis loops of the PZT capacitors under various compressive and tensile bending radii (R). **Figure 7c** shows constant P_{sat}, P_r, E_c and capacitance values within experimental errors under different bending radius. The corresponding nominal strain values estimated by $S = \left(\frac{t_f + t_S}{2R}\right)\left(\frac{1+2\eta+\chi\eta^2}{(1+\eta)(1+\chi\eta)}\right)$ where $\eta = t_f / t_S$, $\chi = Y_f / Y_S$, Y_f is Young's modulus of the PZT layer and Y_S is Young's modulus of the mica are also marked. These results suggest that the PZT thin film capacitor maintains stable electrical properties under mechanical constraints required for the flexible electronics device applications, which was also checked by Raman spectroscopy[20].

The well-saturated and symmetric polarization-electric field (P-E) hysteresis loops and the capacitance-electric field (C-E) with the "butterfly" curves of the heterostructure measured at 1 MHz and temperatures ranging from 25-175 °C for a new device are shown in **Figure 8a and 8b**, respectively. This ferroelectric capacitor exhibits constant saturation polarization (P_{sat}), a remnant polarization (P_r), a coercive field (E_c) and capacitance in a wide temperature range as shown in **Figure 8c**. The heterostructure also maintains high retention and endurance at room temperature as well as at 100 °C[20]. These results imply that the PZT/mica heterostructure can have potential applications in high-temperature electronic devices.

A series of cyclability tests were carried out to validate PZT/mica heterostructures for practical applications. **Figure 9** shows P-E loops before and after 1000 bending cycles in both tensile and compressive strain states. The P-E loops at different bending modes are displaced vertically for the sake of convenience. It is noteworthy that the heterostructure retains its ferroelectric behavior even after 1000 bending cycles at a bending radius of 5 mm irrespective of the nature bending strain.

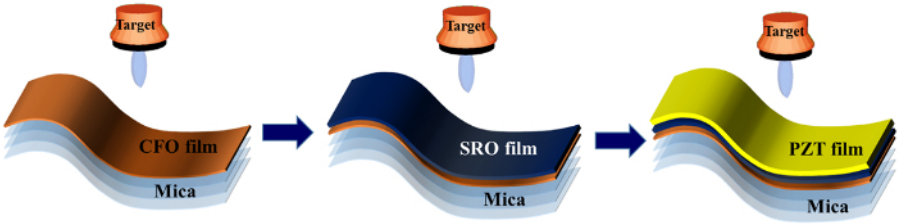

Figure 1. The growth scheme of a flexible memory element on mica. Evacuate the chamber to a base pressure (~10^{-6} Torr) and raise the sample temperature to 590 °C. Adjust the oxygen pressure to 50 mTorr to grow the CFO. Increase the temperature to 680 °C and adjust the oxygen pressure to 100 mTorr to grow the SRO. Decrease the temperature to 650 °C and adjust the oxygen pressure to 100 mTorr to grow the PZT. Please click here to view a larger version of this figure.

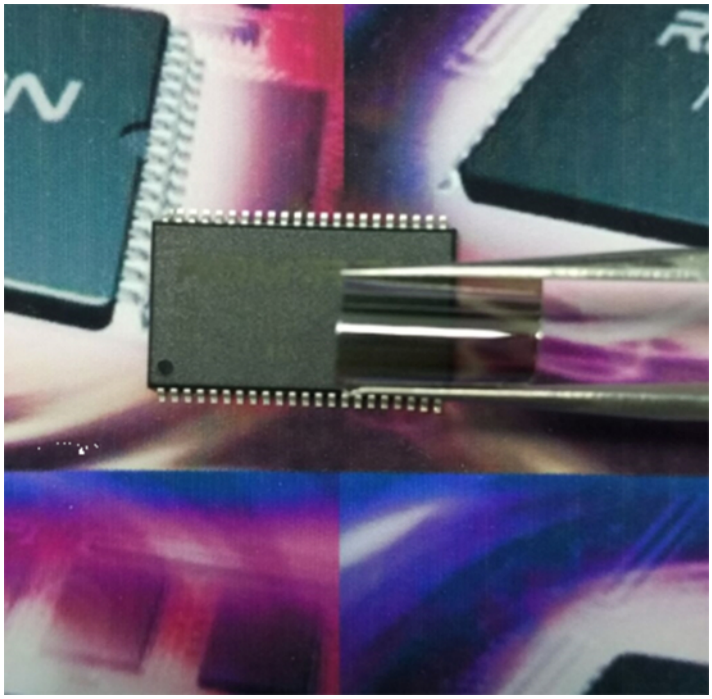

Figure 2. The photograph of a flexible memory element on mica. The flexible memory element can be bent easily. Please click here to view a larger version of this figure.

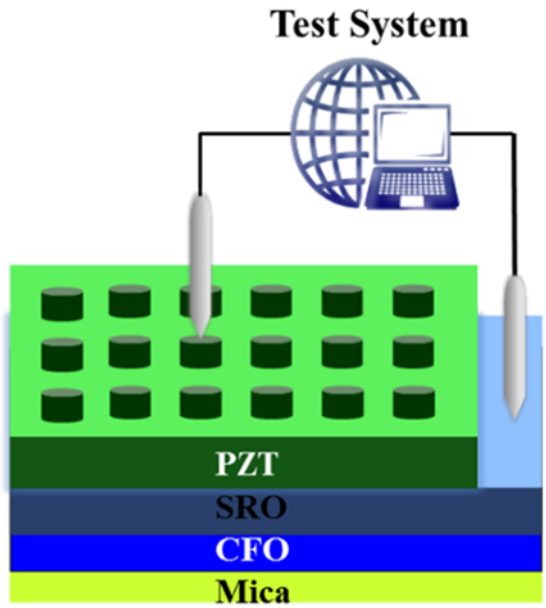

Figure 3.The schematic configuration for measuring P-E hysteresis loops and C-E curve. Contact the SRO bottom electrode using one probe, while the other probe contacts the Pt top electrodes on the films to measure the electronic properties of the PZT thin film. Please click here to view a larger version of this figure.

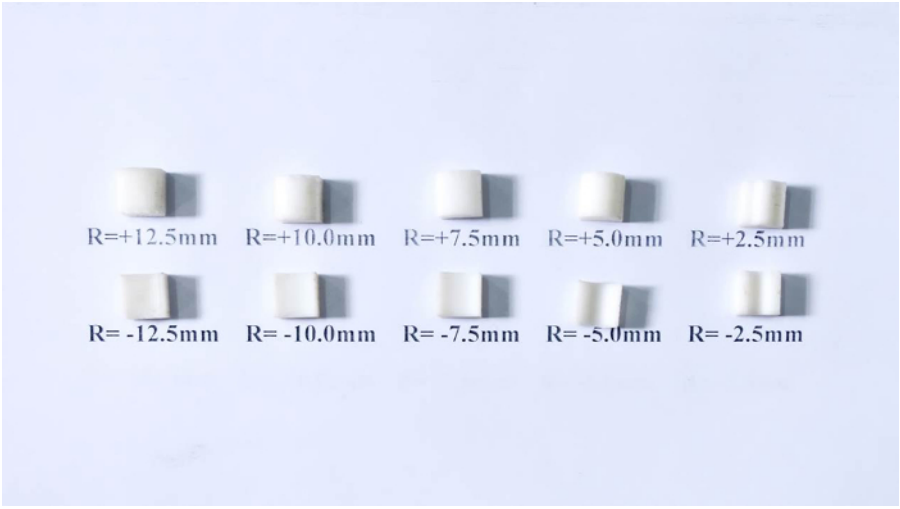

Figure 4. Molds with different fixed bending radii (R). The bending mold designs were made/drawn using autoCAD and printed using a 3D printer. These molds of fixed bending radii (R) induce the reported compressive and tensile bending strains (R = ±12.5 mm, ±10.0 mm, ±7.5 mm, ±5.0 mm, ±2.5 mm, the positive (negative) sign corresponds to tensile (compressive) strain that the heterostructures undergo when mounted on them). Please click here to view a larger version of this figure.

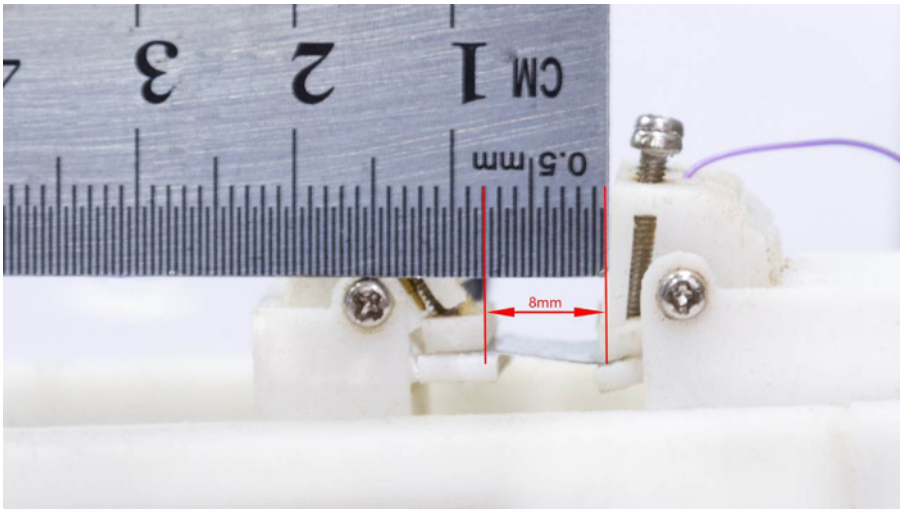

Figure 5. Bending stage to perform bending cycles test. The heterostructure length (C) is measured by a rule in unbent state. For the bending cycle measurement, use a computer-aided home built bending setup. The bending stage consists of two arms with grooves to hold thin sheets. One arm is fixed while the other arm can be moved to bend a thin sheet with a stepper motor interfaced with the computer. Please click here to view a larger version of this figure.

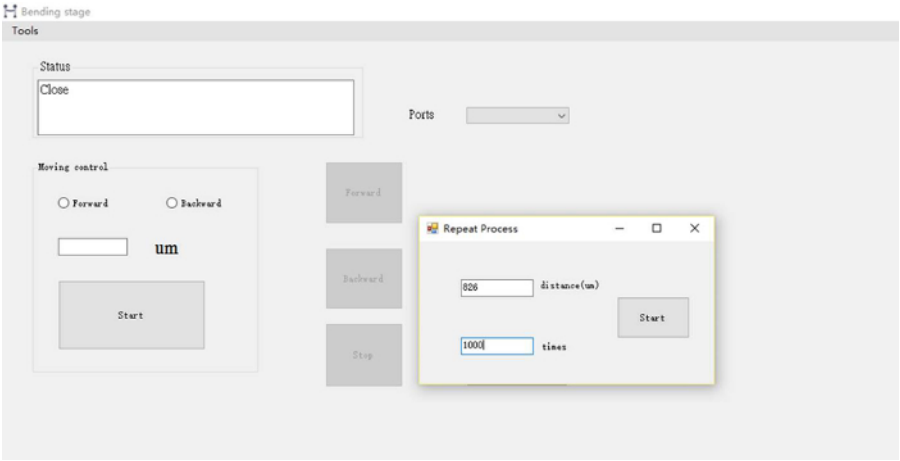

Figure 6. Program protocol to perform bending tests. Use a computer-aided home built bending setup to control the movement of the motor. The setup allows the length of the sample to be bent by providing the displacement as small as 1 µm on the bending stage. One can set the bending radii (see 2.3.4) as well as perform bending cycles. Please click here to view a larger version of this figure.

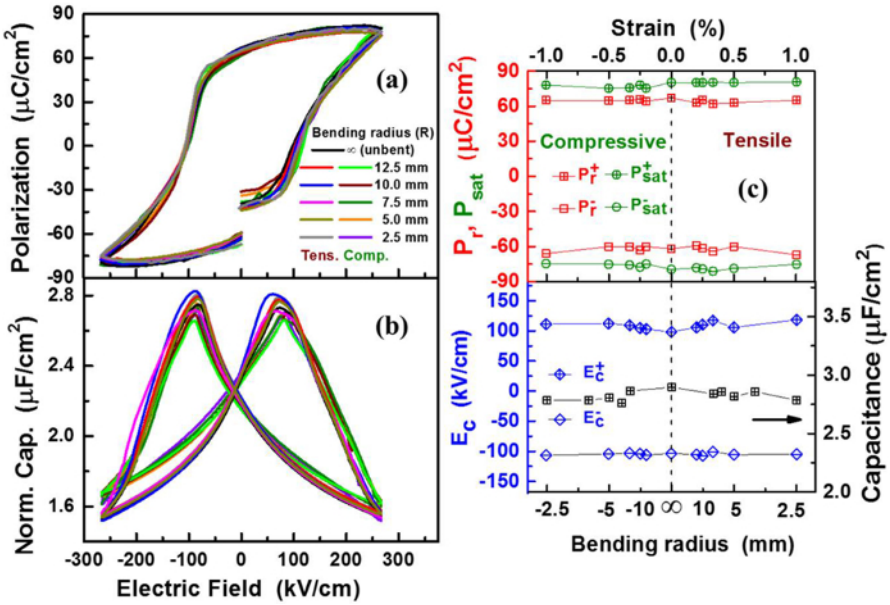

Figure 7. Ferroelectric properties under different bending radii. Electric field dependence of (**a**) polarization and (**b**) capacitance under various tensile and compressive bending radii. (**c**) Saturation polarization (P_{sat}), remnant polarization (P_r), coercive field (E_c) and capacitance as a function of bending radius. Corresponding strain values are also indicated (see text). This Figure has been modified with permission[20]. Please click here to view a larger version of this figure.

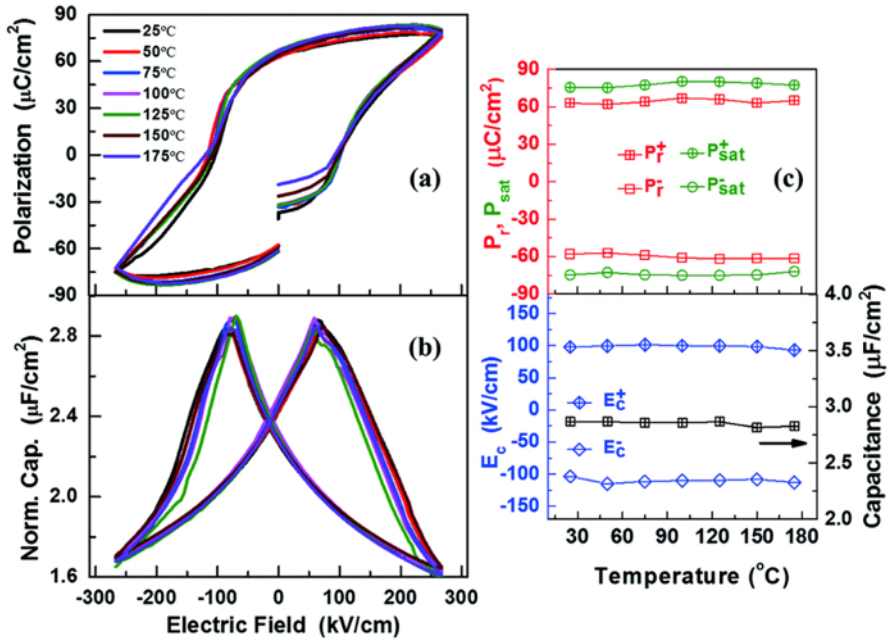

Figure 8. Ferroelectric properties under high temperature. Electric field dependence of (**a**) polarization and (**b**) capacitance at different temperatures. (**c**) Thermal evolution of P_{sat}, P_r, E_c and capacitance. This **Figure** has been modified with permission[20]. Please click here to view a larger version of this figure.

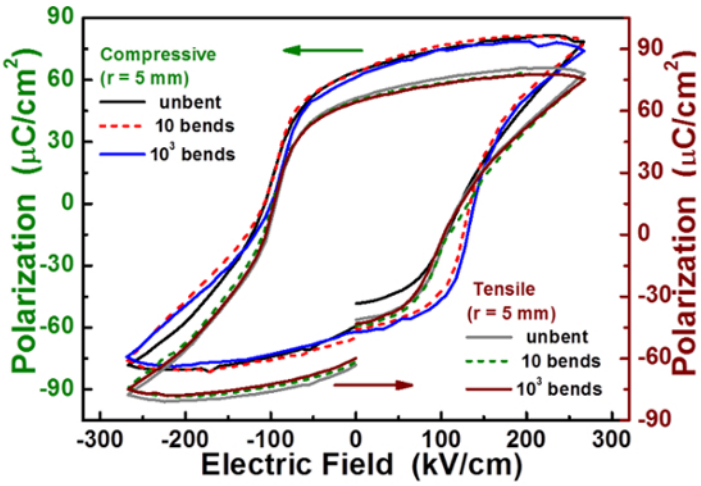

Figure 9. Ferroelectric properties after bending cycles. P-E hysteresis loops under tensile and compressive bending radius of 5 mm before and after 10 to 1000 bending cycles. This Figure has been modified with permission[20]. Please click here to view a larger version of this figure.

Discussion

The key step in the fabrication of ferroelectric elements lies in the use of a clean and even/flat substrate surface. Though freshly cleaved mica surface is atomically smooth, it is necessary to pay attention to preventing surfaces from suffering visible splintering, split layers, cracks, inclusions, *etc.* After deposition of the PZT layer, the sample was cooled under a high oxygen pressure (200-500 Torr) to reduce the oxygen vacancies. *Ex situ* top platinum electrodes were deposited via a predefined mesh to form many Pt/PZT/SRO capacitor elements. To carry out bending tests, the sample was attached to a piece of paper of similar dimensions to enable an easy transfer of the sample between different molds. The molds used to mechanically strain the sample under compressive or tensile states were printed by a 3D printer. During the cycling tests, both ends of the sample were held firmly so as to avoid slipping of mica layers.

However, the inherent small area of uniformity of the PLD technique restricts its applicability in large scale production. The process to choose a good piece of mica without cracks is also time-consuming. Mica cannot be stretched and compressed, and accordingly the devices grown on mica cannot be stretched or compressed, too. A lot of materials grown on mica need a buffer layer to get a good-quality film, which increases the complexity for the production process. These inherent issues restrict the development of flexible devices. Thus, it is necessary to understand in detail the mechanisms governing the nucleation and growth during van der Waals epitaxy and electronic coupling across van der Waals-heterointerfaces in order to circumvent this these issues.

Currently employed strategies for realizing flexible NVME include use of a polymer substrate, thinning of substrate or epitaxial-transfer technique. Though polymer substrates exhibit excellent mechanical compliance, their low temperature stability affects the device performance in a negative way. Also, thinning substrate[8] or epitaxial growth and subsequent transfer on flexible polymer substrate[15] involves a multistep tedious process. The van der Waals epitaxy involving mica[22,23] not only lessens the lattice and thermal matching conditions but also relieves the substrate clamping effect, beneficial for realizing epitaxial systems with performance metrics comparable to single crystalline bulk counterparts as reflected in PZT/mica. Furthermore, 2D layered mica substrate gives the advantage of realizing free-standing-like memory elements that maintain robust ferroelectric behavior against mechanical and thermal constraints. The PZT/mica system possesses the best performance among all the flexible memory elements to date[20], which circumvents the issues of various approaches stated above.

The transparency of mica can be exploited to achieve transparent NVME. Due to the nature of (quasi) van der Waals epitaxy, the material database can be expanded beyond the limited material combinations inherent to conventional epitaxy. It is anticipated that van der Waals epitaxy on mica will trigger substantial research interest in the design and development of next generation of flexible electronic devices.

Disclosures

The authors have no competing financial interests to disclose.

Acknowledgements

This work was supported by National Natural Science Foundation of China (Grant Nos. 11402221 and 11502224), the State Key Laboratory of Intense Pulsed Radiation simulation and effect (SKLIPR1513) and the Hunan Provincial Key Research and Development Plan (No. 2016WK2014).

References

1. Kim, W. Y., Lee, H. C. Stable ferroelectric poly (vinylidene fluoride-trifluoroethylene) film for flexible nonvolatile memory application. *IEEE Electron Device Letters.* **33** (2) 260-262 (2012).
2. Mao, D., Quevedo-Lopez, M. A., Stiegler, H., Gnade, B. E., Alshareef, H. N. Optimization of poly(vinylidene fluoride-trifluoroethylene) films as non-volatile memory for flexible electronics. *Organic Electronics.* **11** (5) 925-932 (2010).
3. Lee, G. G. *et al.* The flexible non-volatile memory devices using oxide semiconductors and ferroelectric polymer poly(vinylidene fluoride-trifluoroethylene). *Applied Physics Letters.* **99** (1) 012901-012903 (2011).
4. Kim, R. H. *et al.* Non-volatile organic memory with sub-millimeter bending radius. *Nature Communications.* **5** 3583-3594 (2014).
5. Liu, J. *et al.* Fabrication of Flexible, All-Reduced graphene oxide non-volatile memory devices. *Advanced Materials.* **25** (2) 233-238 (2013).
6. Ji, Y. *et al.* Stable switching characteristics of organic nonvolatile memory on a bent flexible substrate. *Advanced. Materials.* **22** (28) 3071-3075 (2010).
7. Ghoneim, M. T. *et al.* Thin PZT-based ferroelectric capacitors on flexible silicon for nonvolatile memory applications. *Advanced Electronic Materials.* **1** (6) 1500045-1500054 (2015).
8. Ghoneim, M. T., Hussain, M. M. Study of harsh environment operation of flexible ferroelectric memory integrated with PZT and silicon fabric. *Applied. Physics. Letters.* **107** (5) 052904-052908 (2015).
9. Zuo, Z. *et al.* Preparation and ferroelectric properties of freestanding $Pb(Zr,Ti)O_3$ thin membranes. *Journal of Physics D: Applied Physics.* **45** (18) 185302-185306 (2012).
10. Kingon, A. I., Srinivasan, S. Lead zirconate titanate thin films directly on copper electrodes for ferroelectric, dielectric and piezoelectric applications. *Nature Materials.* **4** (3) 233-237 (2005).
11. Shelton, C. T., Gibbons, B. J. Epitaxial $Pb(Zr,Ti)O_3$ thin films on flexible substrates. *Journal of the American Ceramic Society.* **94** (10) 3223-3226 (2011).
12. Rho, J. *et al.* $PbZr_xTi_{1-x}O_3$ Ferroelectric thin-film capacitors for flexible nonvolatile memory applications. *IEEE Electron Device Letters.* **31** (9) 1017-1019 (2010).
13. Bretos, I. *et al.* Activated Solutions Enabling Low-Temperature processing of functional ferroelectric oxides for flexible electronics. *Advanced Materials.* **26** (9) 1405-1409 (2014).
14. Tsagarakis, E. D., Lew, C., Thompson, M. O., Giannelis, E. P. Nanocrystalline barium titanate films on flexible plastic substrates *via* pulsed laser annealing. *Applied Physics Letters.* **89** (20) 202910-202912 (2006).
15. Bakaul, S. R. *et al.* High speed epitaxial perovskite memory on flexible substrates. *Advanced Materials.* **29** (11) 1605699-1605703 (2017).
16. Li, C. I. *et al.* Van der Waal epitaxy of flexible and transparent VO_2 film on muscovite. *Chemistry of Materials.* **28** (11) 3914-3919 (2016).
17. Ma, C. H. *et al.*Van der Waals epitaxy of functional MoO_2 film on mica for flexible electronics. *Applied Physics Letters.* **108** (25) 253104-253108 (2016).
18. Bitla, Y. *et al.* Oxide heteroepitaxy for flexible optoelectronics. *ACS Applied Materials & Interfaces.* **8** (47), 32401-32407 (2016).
19. Wu, P. C. *et al.* Heteroepitaxy of Fe_3O_4/muscovite: A new perspective for flexible spintronics. *ACS Applied Materials & Interfaces.* **8** (49) 33794-33801 (2016).
20. Jiang, J. *et al.* Flexible ferroelectric element based on van der Waals heteroepitaxy. *Science Advances.* **3** (6), e1700121-e1700128 (2017).
21. Amrillah, T. *et al.* Flexible multiferroic bulk heterojunction with giant magnetoelectric coupling *via* van der waals epitaxy. *ACS Nano.* **11** (6), 6122-6130 (2017).
22. Bitla, Y., Chu, Y. H. MICAtronics: A new platform for flexible X-tronics, *Flat Chem.* **3** 26-42 (2017).
23. Chu, Y. H. Van der Waals oxide heteroepitaxy, *Quantum Materials.* **2** (1) 67-71 (2017).

